Int. J. Heat Mass Transfer. Vol. 34, No. 8, pp. 1991–1998, 1991
Printed in Great Britain

0017–9310/91 $3.00 + 0.00

An experimental study on the spanwise eddy diffusivity of heat in a flat-plate turbulent boundary layer

H. MAEKAWA,† Y. KAWADA,‡ M. KOBAYASHI† and H. YAMAGUCHI§

† Faculty of Engineering, Niigata University, Ikarashi 2-nocho, Niigata 950-21, Japan
‡ Nagaoka College of Technology, Nishikatakai-machi, Nagaoka 940, Japan
§ Kamakura Works, Mitsubishi Electric Corporation, Kamimachiya, Kamakura 247, Japan

(*Received* 29 *June* 1990 *and in final form* 19 *September* 1990)

Abstract—A flat-plate turbulent boundary layer with a constant temperature gradient in the spanwise direction is investigated experimentally to examine distribution characteristics of the spanwise eddy diffusivity of heat. The working fluid is air with a Prandtl number of 0.71. According to the experimental results, the ratio of this eddy diffusivity of heat to the usual kinematic eddy viscosity presents distinctive properties in the immediate vicinity of the wall, the remaining part of the wall region, and the outer region.

INTRODUCTION

ALTHOUGH former experiments and analyses on turbulent thermal boundary layers have been performed mostly under the condition that the velocity and temperature fields are simultaneously two-dimensional, there are many practical situations where the thermal boundary conditions vary in the spanwise direction. In order to analyze such problems using the eddy-diffusivity concept, some reasonable closure expressions should be prepared not only for the kinematic eddy viscosity and the wall-normal eddy diffusivity of heat but also for the spanwise eddy diffusivity of heat. Nevertheless, there exist little accurate experimental data on the eddy diffusivity of heat of the latter type at present. The aim of the present study is to fill up this unexplored area with reliable experimental data.

The first cognition that the wall-normal and spanwise eddy diffusivities of heat at the same point are not necessarily equal is due to Black and Sparrow [1], who performed an experimental investigation, supported by analysis, on non-axisymmetric heat transfer in a circular pipe. Ever since, a series of experiments conducted by Quarmby and Quirk [2] have been the only attempts to measure the circumferential eddy diffusivity of a passive scalar. They measured distributions of nitrous oxide concentration and temperature downstream of non-axisymmetric sources in a circular pipe, and found distribution characteristics of the circumferential eddy diffusivity by analyzing their experimental values with the transport equation for the passive scalar. However, since this kind of analysis requires complicated calculations involving differentiations up to the second order, their final results inevitably contain extremely wide scatter, and thus they are insufficient in accuracy for the purpose of establishing the aforementioned closure expression.

In the present study, a flat-plate turbulent boundary-layer flow of air with a constant spanwise temperature gradient is investigated experimentally. The distribution of the spanwise eddy diffusivity of heat is obtained directly by measuring the corresponding component of turbulent heat flux, and is compared with that of the kinematic eddy viscosity measured in parallel. The mean temperature gradient imposed in the present experiment is indeed artificial, but it brings about an advantage that all turbulence statistics become uniform in the spanwise direction. This makes it easy to obtain basic experimental data which are helpful in examining various closure models for turbulent heat transport.

EXPERIMENTAL SETUP AND MEASUREMENTS

The principal part of the experimental setup used in the present study is illustrated in Fig. 1. This part is incorporated into a closed-circuit wind tunnel, and is installed horizontally. After passing through a contraction and a preheater controlled by an automatic temperature regulator, air flows with uniform velocity and temperature into the heating section. In the heating section, the duct made of plywood, 300 mm high and wide, and 500 mm long, is divided into ten equal channels by 2 mm thick aluminum plates parallel to each other. Rod heaters each rated at 444 W are arrayed, 12 to every channel, perpendicularly to the flow. They are connected to a constant-voltage power source via a turnover switch and an induction regulator so that the flow with a constant temperature gradient or the isothermal flow at a specified constant temperature can be produced at will. The temperature gradient is realized by charging the heaters with electricity as an arithmetical progression with a common

NOMENCLATURE

a	thermal diffusivity
C	empirical constant
C_D	dimensionless coefficient
C_f	skin-friction coefficient
e_c	voltage fluctuation across the cold wire
e_h	voltage fluctuation across the hot wire
H	channel width
k	turbulent kinetic energy
n	empirical constant
Re_m	momentum thickness Reynolds number, $U_\infty \delta_m / \nu$
Re_x	Reynolds number, $U_\infty x/\nu$
r_0	inside radius
$s_{c\theta}$	sensitivity of the cold wire to θ
s_{hw}	sensitivity of the hot wire to w
$s_{h\theta}$	sensitivity of the hot wire to θ
U	streamwise mean velocity
U_∞	free-stream velocity
u	streamwise velocity fluctuation
u_τ	friction velocity, $\sqrt{(\tau_w/\rho)}$
u^+	dimensionless velocity, U/u_τ
v	wall-normal or radial velocity fluctuation
w	spanwise or circumferential velocity fluctuation
x	distance from the nose
y	distance from the wall
y^+	dimensionless distance, $u_\tau y/\nu$
z	spanwise coordinate.

Greek symbols

δ	boundary layer thickness
δ_m	momentum thickness
ε	rate of dissipation of k
ε_{hy}	wall-normal or radial eddy diffusivity of passive scalar
ε_{hz}	spanwise or circumferential eddy diffusivity of passive scalar
ε_m	kinematic eddy viscosity
Θ	mean temperature
Θ_0	Θ in the x–y plane
θ	temperature fluctuation
ν	kinematic viscosity
ρ	density
τ_w	wall shear stress
ϕ	yaw angle of the hot wire
ψ	stream function
ψ^*	dimensionless stream function, ψ/ν.

Superscripts and subscripts

$\overline{\ }$	time mean
$+$	$\phi = \pi/4$
$-$	$\phi = -\pi/4$.

difference of unity. It is directed upward to prevent the secondary flow due to buoyancy from occurring. To reduce the turbulence generated in the heating section, 40-mesh stainless-steel screens are located 650 and 725 mm downstream of the heating section. The flat plate is an acrylic plastic plate, 5 mm thick, 300 mm high, and 2100 mm long, with a chisel-shaped leading edge. It is mounted in the vertical center plane of the test section 600 mm from the downstream screen. The boundary layer along the flat plate is tripped with a steel wire of 1 mm in diameter adhered 50 mm downstream from the nose. The duct of the test section is made of plywood. Its height is the same as in the heating section, but its width is adjusted to eliminate the streamwise pressure gradient.

In the Cartesian coordinate system shown in Fig. 1, x is measured in the downstream direction from the nose of the flat plate. y is the distance from the wall, and z is measured upward from the centerline of the flat plate.

Measurements were made mainly on the streamwise mean velocity U, the mean temperature Θ, the kinematic turbulent shear stress $-\overline{uv}$ and the spanwise thermometric turbulent heat flux $\overline{w\theta}$ in the vicinity of the x–y plane. During the measurements, the free-stream velocity U_∞ was maintained at 9.1 m s^{-1}, and the mean temperature on the x–y plane Θ_0 at 314.2 K. The corresponding unit Reynolds number U_∞/ν was 5.33×10^5 m^{-1}.

The mean velocity and the turbulent stresses were

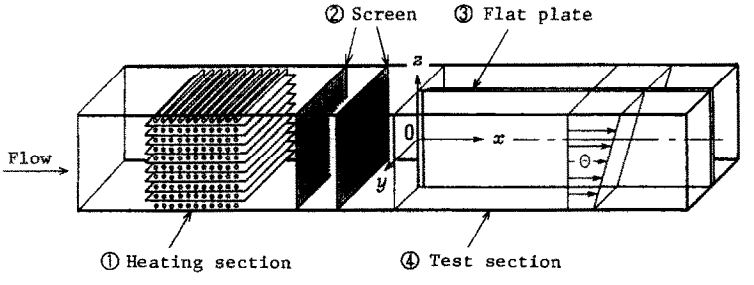

FIG. 1. Principal part of the experimental setup.

measured with hot-wire anemometers, switching the flow into the isothermal. The mean temperature was measured with a platinum cold wire.

Two methods were adopted in the measurements of the spanwise turbulent heat flux. In the first method, two tungsten hot wires of 2.6 μm in diameter, 0.7 and 1.0 mm long, were used separately. They were placed parallel to the wall, and were operated at a relatively low over-heat ratio. After measuring the variances of voltage fluctuations $(\overline{e_h^2})_\pm$ at yaw angles of $\phi = \pm\pi/4$ repeatedly, the experimental values for $\overline{w\theta}$ were obtained according to the following equation:

$$(\overline{e_h^2})_+ - (\overline{e_h^2})_- = 4s_{hw}s_{h\theta}\overline{w\theta} \tag{1}$$

where s_{hw} and $s_{h\theta}$ represent sensitivities of the hot wire at $\phi = \pi/4$ to the spanwise velocity fluctuation w and the temperature fluctuation θ, respectively. In the second method, use was made of a two-wire probe in which a tungsten hot wire of 2.6 μm in diameter, 0.4 mm long, and a platinum cold wire of 0.63 μm in diameter, 1.3 mm long, were arrayed parallel to each other with a lateral space of about 0.3 mm. The hot wire was placed parallel to the wall, and was operated at an over-heat ratio as high as possible. The covariances of voltage fluctuations $(\overline{e_h e_c})_\pm$ were measured at $\phi = \pm\pi/4$ alternately, and the experimental values of $\overline{w\theta}$ were obtained according to the following equation:

$$(\overline{e_h e_c})_+ - (\overline{e_h e_c})_- = 2s_{hw}s_{c\theta}\overline{w\theta} \tag{2}$$

where $s_{c\theta}$ is the sensitivity of the cold wire to the temperature fluctuation.

Of course, the first method is superior to the second in the sense that the error arising from the spatial resolution power can be reduced. On the other hand, in the case of the second method, extra terms other than $\overline{w\theta}$ which are contained in the covariances of voltage fluctuations are only those of the streamwise turbulent heat flux $\overline{u\theta}$ and the temperature variance $\overline{\theta^2}$. However, $\overline{u\theta}$ is not produced theoretically in the boundary layer of the present experiment. Moreover, the high over-heat ratio of the hot wire makes the contribution of $\overline{\theta^2}$ to the covariances sufficiently small. Accordingly, accidental errors contained in the covariances of voltage fluctuations are not much magnified through the subtraction in equation (2). Although equations (1) and (2) are similar in form, the second method is superior to the first in this respect.

The variances and covariances of voltage fluctuations were numerically obtained from 4.10×10^5 sets of data sampled at a rate of 9 kHz over a 45 s period, using an on-line real time system developed by the present authors. The sensitivities to velocity fluctuations were assumed to be equal to the statically calibrated values. The sensitivities to temperature fluctuation were estimated by multiplying the statically calibrated values by certain factors. These factors stand for the gain for the frequency range where only the wires respond to the temperature fluctuation and the remaining parts of the probe cease to respond. A transfer function derived by the present authors [3] was used in evaluating them.

EXPERIMENTAL RESULTS AND DISCUSSION

Irrespective of the existence of the temperature gradient, the velocity boundary layer was completely two-dimensional at least in the region of -50 mm $< z < 50$ mm, and the free-stream velocity was substantially constant in the region of $x > 600$ mm.

The friction velocity u_τ which becomes necessary for the data arrangement described in the following was calculated from the streamwise variation in the momentum thickness δ_m using the following equation:

$$C_f = 2\left(\frac{u_\tau}{U_\infty}\right)^2 = 2\frac{d\delta_m}{dx} \tag{3}$$

where C_f is the skin-friction coefficient. Equation (3) is identical with the momentum integral equation. Figure 2 shows the values of C_f obtained in this manner as a function of momentum thickness Reynolds number $Re_m = U_\infty\delta_m/\nu$, and indicates that the present experimental results are consistent with those obtained by Murlis *et al.* [4].

All the experimental data presented in the following were acquired at two measuring stations, $x = 900$ and 1500 mm, which correspond to momentum thickness Reynolds numbers of 1.15×10^3 and 1.75×10^3.

The mean-velocity distributions plotted in the semi-logarithmic form are shown in Fig. 3, where $u^+ = U/u_\tau$ and $y^+ = u_\tau y/\nu$. As shown in the figure, the mean-velocity distributions in the inner layer agree fairly well with the universal velocity distribution with generally accepted constants.

The spanwise distributions of the mean temperature for several fixed values of y are shown in Fig. 4. This

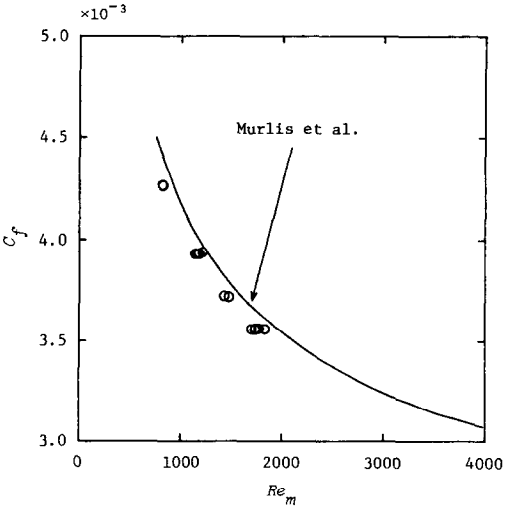

FIG. 2. Variation of the skin-friction coefficient with momentum thickness Reynolds number.

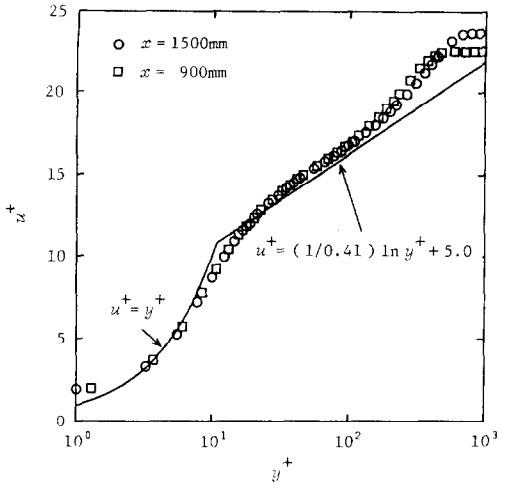

FIG. 3. Mean-velocity distribution.

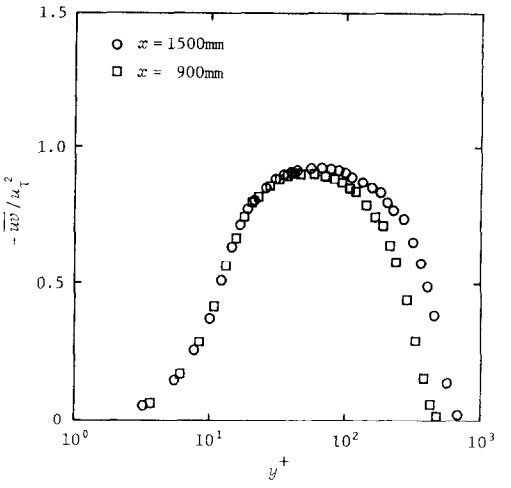

FIG. 5. Distribution of the turbulent shear stress.

figure is for the downstream measuring station, but almost identical distributions were obtained at the upstream measuring station as well. As expected, an accurately linear temperature profile was produced in the central part of the test section, and its gradient was substantially constant independent of the distance from the wall.

The turbulent shear stress distributions in the vicinity of the wall were obtained from the aforecited experimental results on the velocity field, using the following equation:

$$\left(\frac{U_\infty}{u_\tau}\right)^2\left[\frac{\mathrm{d}}{\mathrm{d}Re_x}\left(\frac{u_\tau}{U_\infty}\right)\right]\int_0^{y^+}(u^+)^2\,\mathrm{d}y^+ = \frac{\mathrm{d}u^+}{\mathrm{d}y^+} - \frac{\overline{uv}}{u_\tau^2} - 1 \tag{4}$$

where $Re_x = U_\infty x/\nu$. Equation (4) holds accurately in the inner layer where the mean-velocity distribution can be unified as the 'law of the wall' (see Appendix). In Fig. 5, the turbulent shear stress distributions thus obtained and those measured with a ×-probe are joined at the middle of the inner layer.

Among the three components of turbulent heat flux, only the spanwise component is produced substantially in the boundary layer of the present experiment. Figure 6 shows the distributions of this quantity, which is normalized by the spanwise heat flux at an infinitesimal distance from the wall.

According to Kline *et al.* [5], the streaky structure in the buffer layer has a mean spacing of about 100 in the wall unit ν/u_τ. On the other hand, in the case of the 0.7 mm long hot wire which was used in the measurement of $\overline{w\theta}$, the wire length projected in the streamwise direction was about 12 when measured with the wall unit at $x = 900$ mm. This value may not be necessarily small enough as compared with the

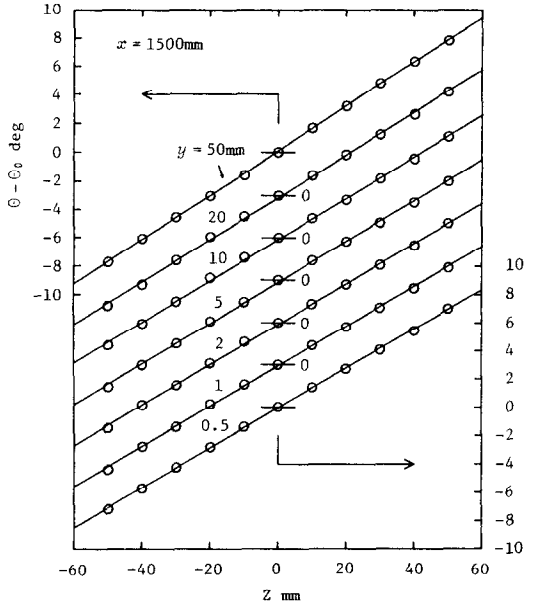

FIG. 4. Spanwise distribution of the mean temperature.

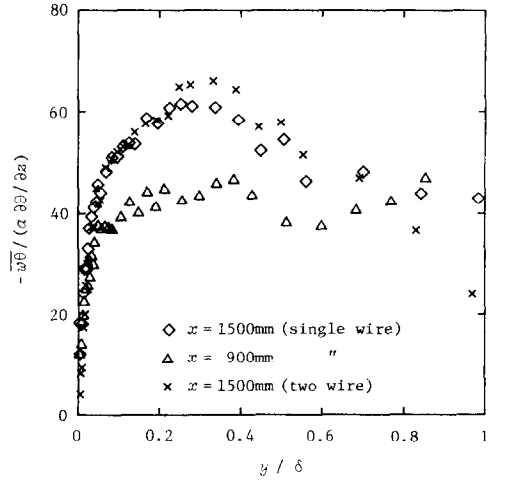

FIG. 6. Distribution of the spanwise turbulent heat flux.

streak spacing, but no significant effect of the wire length was found among the obtained values of $\overline{w\theta}$. Figure 6 indicates that the values of $\overline{w\theta}$ measured with the two-wire probe agree reasonably well with those measured with the single wire.

When the free stream is settled perfectly, the spanwise turbulent heat flux together with its rate of production can be expected to vanish at the outer edge of the boundary layer. Contrary to this expectation, $\overline{w\theta}$ in Fig. 6 maintains a certain level in the outer half of the boundary layer. This is probably because eddies weak in vorticity but large in size existed in the free stream. The relative turbulence intensity $\sqrt{(u^2)}/U_\infty$ was 0.79 and 0.75% at $x = 900$ and 1500 mm, respectively.

The kinematic eddy viscosity ε_m and the spanwise eddy diffusivity of heat ε_{hz} were obtained by substituting the aforecited experimental values into the following definitions:

$$-\overline{uv} = \varepsilon_m \frac{\partial U}{\partial y} \tag{5}$$

$$\overline{w\theta} = -\varepsilon_{hz} \frac{\partial \Theta}{\partial z}. \tag{6}$$

In the wall region, both ε_m/ν and ε_{hz}/ν are functions of y^+. On the other hand, in the outer region where the boundary layer thickness δ represents the characteristic length scale, $\varepsilon_m/(u_\tau\delta)$ and $\varepsilon_{hz}/(u_\tau\delta)$ can be expressed alike as functions of y/δ. These two kinds of functional relationships are shown in Figs. 7 and 8. The distribution of ε_m/ν in the constant-stress layer which was calculated using van Driest's mixing length

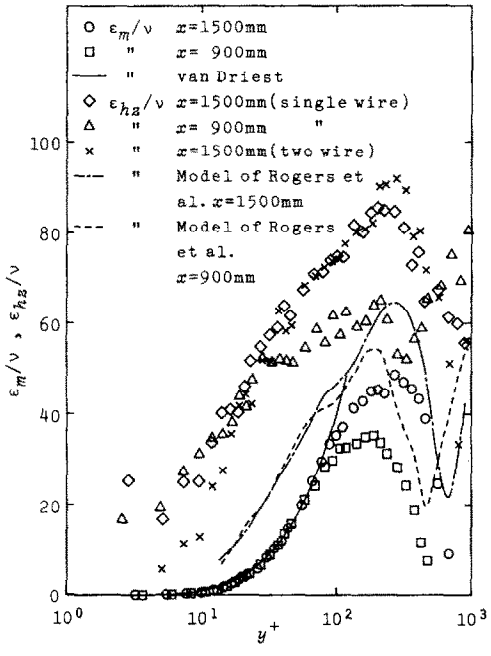

FIG. 7. Distributions of the kinematic eddy viscosity and the spanwise eddy diffusivity of heat in the vicinity of the wall.

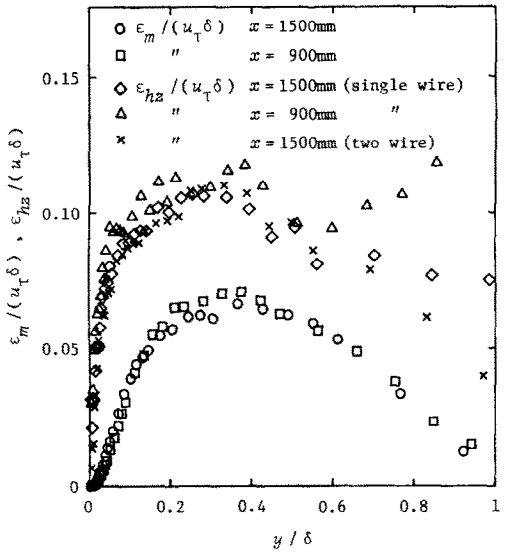

FIG. 8. Distributions of the kinematic eddy viscosity and the spanwise eddy diffusivity of heat over the boundary-layer thickness.

[6] is also shown in Fig. 7. As a matter of course, the experimental and calculated values of ε_m/ν are in good agreement in the vicinity of the wall. The values of ε_{hz}/ν scatter widely, but a certain degree of coherence is clearly observable among them in the vicinity of the wall. Extraordinary behavior of $\varepsilon_{hz}/(u_\tau\delta)$ in the outer half of the boundary layer can be considered to arise from the free-stream turbulence as described above. However, Fig. 8 indicates that this influence does not reach the inner half of the boundary layer.

The distributions of the eddy diffusivity ratio $\varepsilon_{hz}/\varepsilon_m$ plotted against y^+ and y/δ are shown in Figs. 9 and 10, respectively. In the vicinity of the wall, $\varepsilon_{hz}/\varepsilon_m$ increases rapidly, since ε_{hz} approaches zero more slowly than ε_m. However, as the distance from the wall increases, the distributions of ε_m and ε_{hz} become similar, and, as

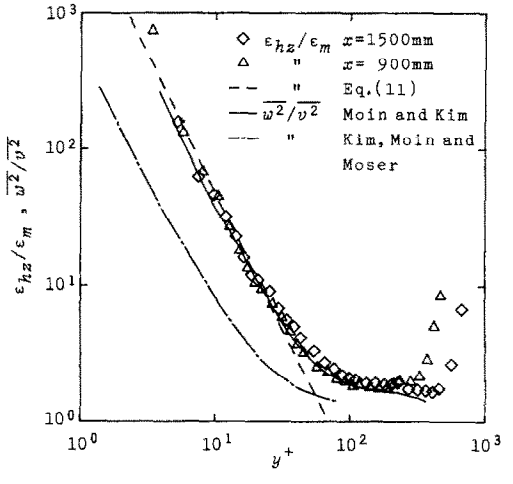

FIG. 9. Distribution of the eddy-diffusivity ratio in the vicinity of the wall.

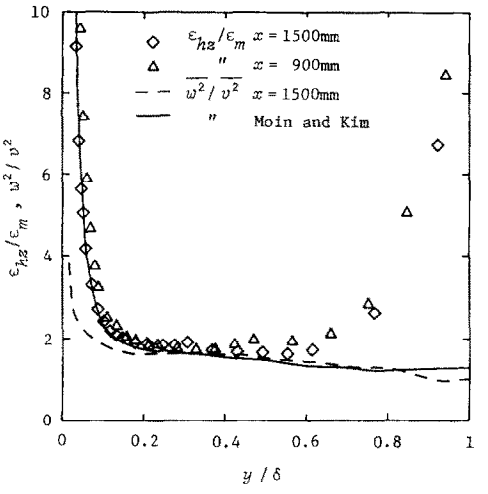

FIG. 10. Distribution of the eddy-diffusivity ratio over the boundary-layer thickness.

a result, $\varepsilon_{hz}/\varepsilon_m$ approaches a constant value. Such behavior of $\varepsilon_{hz}/\varepsilon_m$, especially that shown in Fig. 10 is qualitatively consistent with the results obtained by Quarmby and Quirk [2]. As has already been mentioned above, they measured the circumferential and radial eddy diffusivities of passive scalar, ε_{hz} and ε_{hy}, in a circular pipe of r_0 in inside radius, and expressed the results as a functional relationship between $\varepsilon_{hz}/\varepsilon_{hy}$ and y/r_0.

Launder [7] considered the behavior of $\varepsilon_{hz}/\varepsilon_{hy}$ from a view point of scalar flux balance. Postulating the local-equilibrium region at high Reynolds number and assuming the pressure-scalar-gradient correlation to be simply in proportion to the corresponding scalar flux, he derived the following relation:

$$\frac{\varepsilon_{hz}}{\varepsilon_{hy}} = \frac{\overline{w^2}}{\overline{v^2}} \tag{7}$$

where $-\overline{w^2}$ and $-\overline{v^2}$ are the kinematic turbulent normal stresses acting in the circumferential and radial directions, respectively. When the concept of turbulent Prandtl number $\varepsilon_m/\varepsilon_{hy}$ is introduced, his idea can be extended to the case of $\varepsilon_{hz}/\varepsilon_m$, almost automatically without going so far as to consider the shear stress balance instead of the wall-normal scalar flux balance. In fact, from a number of former experimental studies as well as a direct numerical simulation recently performed by Kim and Moin [8], it is generally accepted that the turbulent Prandtl number takes values close to unity over the entire region of the inner layer. Accordingly, it is possible to rewrite equation (7) as

$$\frac{\varepsilon_{hz}}{\varepsilon_m} = \frac{\overline{w^2}}{\overline{v^2}}. \tag{8}$$

Launder verified equation (7) by quoting the aforementioned Quarmby and Quirk's results on $\varepsilon_{hz}/\varepsilon_{hy}$ and Laufer's experimental data on $\overline{v^2}$ and $\overline{w^2}$ [9]. Figure 10 compares the present experimental results for $\varepsilon_{hz}/\varepsilon_m$ and $\overline{w^2}/\overline{v^2}$. The agreement between these quantities is solid in the turbulent region of the inner layer.

Recently, in dealing with anisotropic diffusion of heat in a two-dimensional channel, Kasagi *et al.* [10] expressed the ratio of ε_{hz} to the wall-normal eddy diffusivity of heat ε_{hy} with both a simple and rational empirical formula as follows:

$$\frac{\varepsilon_{hz}}{\varepsilon_{hy}} = \left(\frac{y^+}{C}\right)^{-2} + \left(\frac{2y}{H}\right)^n \tag{9}$$

where C and n are empirical constants, and H is the channel width. They chose 140 and 0.1 as the optimum values for C and n, respectively, and succeeded in predicting the mean temperature distributions consistent with their own experimental results. One of the essential points of their proposition is to combine the aforementioned Launder's conjecture with the asymptotic behavior of turbulence in the immediate vicinity of the wall:

$$\frac{\overline{w^2}}{\overline{v^2}} \propto (y^+)^{-2}. \tag{10}$$

By determining the optimum value for C from the present experimental results, we obtained

$$\frac{\varepsilon_{hz}}{\varepsilon_m} = \left(\frac{y^+}{70}\right)^{-2}. \tag{11}$$

For the sake of comparison with the experimental results, equation (11) is shown with a dotted line in Fig. 9. The value of C determined by Kasagi *et al.* seems to be indeed excessive as compared with the present experimental value. However, the essential feature of their proposition which is presented by the first term on the right-hand side of equation (9) is definitely confirmed in the present experimental results as well.

On the statistical properties of wall turbulence, especially on those in the immediate vicinity of the wall which involve great difficulties in accurate measurement, valuable data were published by Moin and Kim [11] and Kim *et al.* [12]. Moin and Kim made a numerical investigation on a fully-developed turbulent flow in a two-dimensional channel by means of a large-eddy simulation. Kim *et al.* performed a direct numerical simulation on the same flow. In Fig. 9, values of $\overline{w^2}/\overline{v^2}$ calculated from their results are compared with $\varepsilon_{hz}/\varepsilon_m$. Here it is necessary to note that Moin and Kim's original data are those for the resolvable field corresponding to large-scale eddies, and thus they contain no contribution from the subgrid-scale motion. In addition, the local-equilibrium condition which was assumed in the derivation of equation (7) does not hold in the immediate vicinity of the wall. Nevertheless, the agreement of $\overline{w^2}/\overline{v^2}$ of the resolvable field with $\varepsilon_{hz}/\varepsilon_m$ is striking not only in the turbulent region of the inner layer but also in the immediate vicinity of the wall. No clear reason can be given at present to this agreement in the

immediate vicinity of the wall. However, as a probable reason, it is possible to mention that, of the total amounts of the turbulent shear stress and the turbulent heat flux, fractions produced by large-scale eddies may have extremely longer lifespans than those produced by small-scale eddies.

Rogers *et al.* [13] performed direct numerical simulations on homogeneous turbulent shear flows with mean scalar gradients in each of the three orthogonal directions, and used the results to derive an algebraic model for the turbulent scalar flux. For the case of the present experiment, their model yields

$$\varepsilon_{hz} = \frac{2k/\varepsilon}{C_D}\overline{w^2} \tag{12}$$

where k and ε denote the turbulent kinetic energy per unit mass and its rate of dissipation, respectively. C_D is a dimensionless coefficient which depends on the turbulent Reynolds and Peclet numbers and to which Rogers *et al.* gave a concrete expression. Also included in Fig. 7 are the values of ε_{hz}/ν which are calculated by substituting the present experimental values for k, ε and $\overline{w^2}$ into equation (12). The experimental values for ε were obtained from the one-dimensional power spectra of $\overline{u^2}$ in the inertial subrange according to Lawn's proposal [14]. Figure 7 indicates that the model of Rogers *et al.* underpredicts the magnitude of ε_{hz} over the entire region of the boundary layer.

SUMMARY

The spanwise eddy diffusivity of heat ε_{hz} was measured directly for air in a flat-plate turbulent boundary layer, and was compared with the kinematic eddy viscosity ε_m measured in parallel.

As to the distribution characteristics of the eddy diffusivity ratio $\varepsilon_{hz}/\varepsilon_m$, it is concluded that:

(1) In the immediate vicinity of the wall, $\varepsilon_{hz}/\varepsilon_m$ increases rapidly, and follows asymptotically the -2nd power of the dimensionless distance from the wall.

(2) In the turbulent region of the inner layer, $\varepsilon_{hz}/\varepsilon_m$ agrees closely with the ratio between the turbulent normal stresses acting in the spanwise and wall-normal directions.

(3) In the outer region, $\varepsilon_{hz}/\varepsilon_m$ is sensitive to the free-stream turbulence.

Although conclusions (1) and (2) can be considered to be basically common in all kinds of wall turbulence, it is necessary hereafter to make clear to what degree these universalities hold in the other representative turbulent flows.

REFERENCES

1. A. W. Black and E. M. Sparrow, Experiments on turbulent heat transfer in a tube with circumferentially varying thermal boundary conditions, *Trans. ASME, J. Heat Transfer* **89,** 258–268 (1967).
2. A. Quarmby and R. Quirk, Measurements of the radial and tangential eddy diffusivities of heat and mass in turbulent flow in a plain tube, *Int. J. Heat Mass Transfer* **15,** 2309–2327 (1972).
3. H. Maekawa, M. Kobayashi and K. Yashiro, Frequency response of a constant-temperature hot wire to temperature fluctuations, *JSME Int. J.* **30,** 1783–1789 (1987).
4. J. Murlis, H. M. Tsai and P. Bradshaw, The structure of turbulent boundary layers at low Reynolds numbers, *J. Fluid Mech.* **122,** 13–56 (1982).
5. S. J. Kline, W. C. Reynolds, F. A. Schraub and P. W. Runstadler, The structure of turbulent boundary layers, *J. Fluid Mech.* **30,** 741–773 (1967).
6. E. R. van Driest, On turbulent flow near a wall, *J. Aero. Sci.* **23,** 1007–1011 and 1036 (1956).
7. B. E. Launder, Heat and mass transport. In *Topics in Applied Physics* (Edited by P. Bradshaw), pp. 231–287. Springer, Berlin (1978).
8. J. Kim and P. Moin, Transport of passive scalars in a turbulent channel flow. In *Turbulent Shear Flows 6* (Edited by J.-C. André, J. Consteix, F. Durst, B. E. Launder, F. W. Schmidt and J. H. Whitelaw), pp. 85–96. Springer, Berlin (1984).
9. J. Laufer, The structure of turbulence in fully developed pipe flow, NACA Rep. 1174 (1955).
10. N. Kasagi, R. Kaneko, H. K. Myong and M. Hirata, Anisotropic diffusion of scalar quantities in a two-dimensional turbulent channel flow, Preprint of 24th Natn. Heat Transfer Symp. of Japan, pp. 7–9 (1987), in Japanese.
11. P. Moin and J. Kim, Numerical investigation of turbulent channel flow, *J. Fluid Mech.* **118,** 341–377 (1982).
12. J. Kim, P. Moin and R. Moser, Turbulence statistics in fully developed channel flow at low Reynolds number, *J. Fluid Mech.* **177,** 133–166 (1987).
13. M. M. Rogers, N. N. Mansour and W. C. Reynolds, An algebraic model for the turbulent flux of a passive scalar, *J. Fluid Mech.* **203,** 77–101 (1989).
14. C. J. Lawn, The determination of the rate of dissipation in turbulent pipe flow, *J. Fluid Mech.* **48,** 477–505 (1971).

APPENDIX

Although equation (4) can be derived in several different ways, the derivation described here starts with the streamwise momentum equation in the von Mises coordinate system (x, ψ) as follows:

$$\frac{\partial U}{\partial x} = \frac{\partial}{\partial \psi}\left(\nu U \frac{\partial U}{\partial \psi} - \overline{uv}\right) \tag{A1}$$

where ψ is the stream function defined by

$$\psi = \int_0^y U \, dy. \tag{A2}$$

Integration of equation (A1) yields

$$\frac{\partial}{\partial x}\int_0^{\psi} U \, d\psi = \nu U \frac{\partial U}{\partial \psi} - \overline{uv} - u_\tau^2. \tag{A3}$$

Especially for the boundary layer flow, the dimensionless variable $\psi^* = \psi/\nu$ and others can be introduced to obtain

$$\left(\frac{U_\infty}{u_\tau}\right)^2 \frac{\partial}{\partial Re_x}\left(\frac{u_\tau}{U_\infty}\int_0^{\psi^*} u^+ \, d\psi^*\right) = u^+ \frac{\partial u^+}{\partial \psi^*} - \frac{\overline{uv}}{u_\tau^2} - 1. \tag{A4}$$

Moreover, for the inner layer where the 'law of the wall' can be assumed to hold exactly, equation (A4) simplifies to

$$\left(\frac{U_\infty}{u_\tau}\right)^2\left[\frac{\mathrm{d}}{\mathrm{d}Re_x}\left(\frac{u_\tau}{U_\infty}\right)\right]\int_0^{y^+}(u^+)^2\,\mathrm{d}y^+ = \frac{\mathrm{d}u^+}{\mathrm{d}y^+} - \frac{\overline{uv}}{u_\tau^2} - 1 \quad \text{(A5)}$$

since u^+ and, in its turn

$$\psi^* = \int_0^{y^+} u^+\,\mathrm{d}y^+ \quad \text{(A6)}$$

are functions of y^+ alone.

ETUDE EXPERIMENTALE SUR LA DIFFUSIVITE TURBULENTE LATERALE DE LA CHALEUR DANS UNE COUCHE LIMITE TURBULENTE SUR PLAQUE PLANE

Résumé—On étudie expérimentalement une couche limite turbulente sur plaque plane avec gradient de température uniforme dans la direction transversale, pour examiner les caractéristiques de la diffusivité turbulente latérale de la chaleur. Le fluide de travail est l'air avec un nombre de Prandtl 0,71. Selon les résultats expérimentaux, le rapport de cette diffusivité turbulente de la chaleur à la viscosité turbulente cinématique présente des propriétés particulières au voisinage immédiat de la paroi, dans la région intermédiaire et dans la région extérieure.

EXPERIMENTELLE UNTERSUCHUNG DER VERTEILUNG DER TURBULENTEN TEMPERATURLEITFÄHIGKEIT QUER ZUR STRÖMUNGSRICHTUNG IN EINER TURBULENTEN GRENZSCHICHT AN EINER EBENEN PLATTE

Zusammenfassung—Eine turbulente Grenzschicht mit konstanten Temperaturgradienten senkrecht zur Strömungsrichtung an einer ebenen Platte wird experimentell untersucht. Dabei wird die Verteilung der turbulenten Temperaturleitfähigkeit senkrecht zur Strömungsrichtung bestimmt. Das Arbeitsfluid ist Luft mit einer Prandtl-Zahl von 0,71. Die Ergebnisse zeigen, daß das Verhältnis der turbulenten Temperaturleitfähigkeit zur üblichen turbulenten kinematischen Viskosität ein in jedem Bereich der Grenzschicht typisches, unterscheidbares Verhalten zeigt—sowohl in der unmittelbaren Nähe der Wand, als auch im verbleibenden Teil der Wandregion und in der Außenregion.

ЭКСПЕРИМЕНТАЛЬНОЕ ИССЛЕДОВАНИЕ ТУРБУЛЕНТНОЙ ТЕМПЕРАТУРОПРОВОДНОСТИ В ТУРБУЛЕНТНОМ ПОГРАНИЧНОМ СЛОЕ НА ПЛОСКОЙ ПЛАСТИНЕ

Аннотация—С целью изучения распределения турбулентной температуропроводности проведены экспериментальные исследования турбулентного пограничного слоя на плоской пластине с постоянным продольным температурным градиентом. Рабочей средой являлся воздух с числом Прандтля, равным 0,71. Результаты экспериментов показали, что отношение исследуемой турбулентной температуропроводности к кинематической турбулентной вязкости является различным в непосредственной близости от стенки, во внешнем течении и в промежуточной области.